Study of Morphological and Mechanical Performance of Amine-Cured Glassy Epoxy–Clay Nanocomposites

A. Mouloud,[1] R. Cherif,[1] S. Fellahi,[2] Y. Grohens,[3] I. Pillin[3]

[1]*Polytechnic Military School, B.P 17, EMP, Bordj-El-Bahri, 16111 Algiers, Algeria*
[2]*Plastics and Rubber Engineering Department, Algerian Petroleum Institute, 35000 Boumerdes, Algeria*
[3]*Materials Engineering Laboratory of Bretagne, Research Centre, Rue de Saint Maudé, 56321 Lorient, France*

Received 14 December 2010; accepted 22 August 2011
DOI 10.1002/app.35520
Published online 6 December 2011 in Wiley Online Library (wileyonlinelibrary.com).

ABSTRACT: The effect of three different alkylammonium-modified montmorillonite on morphological and mechanical properties of glassy epoxy-amine nanocomposites is reported. Small amounts of clays <10 phr (part per hundred of resin) were used in each system of nanocomposite. The morphology of the prepared nanocomposites was performed by means of X-ray diffraction and transmission electron microscopy. Differential scanning calorimetry (DSC) was used to investigate the glass transition temperatures (T_g). Mechanical properties were based on tensile characteristics (Young's modulus), impact strength, and fracture toughness. The measured moduli were compared to theoretical predictions. Scanning electron microscopy was used to study the morphological structure of the fracture surfaces of impacted specimens. It was found that at a low content of 2 phr (1.2 wt %) of nanoclays, the impact strength and the fracture toughness were improved by 77 and 90% respectively, comparatively to the neat epoxy, whereas DSC revealed a reduction of the T_g of nanocomposites. © 2011 Wiley Periodicals, Inc. J Appl Polym Sci 124: 4729–4739, 2012

Key words: epoxy nanocomposites; montmorillonite; morphology; impact strength; toughness

INTRODUCTION

Epoxy resins are a major class of thermosetting polymers generally known as materials that provide many desirable properties, and find extensive use in various fields of coating, high-performance adhesives, and other engineering applications. Once cured, they are characterized by high chemical and corrosion resistance as well as good mechanical and thermal properties. However, cured epoxy resins are relatively brittle polymers with poor resistance to crack growth and impact strength, i.e., they exhibit low fracture toughness. Thus, several approaches have been proposed in an effort to improve their performances. Nevertheless, it has been well established for many years that the incorporation of a second microphase of a dispersed rubber or a thermoplastic polymer can increase the toughness, but simultaneously increases the viscosity of the epoxy monomer mixture and reduces the modulus of the cured epoxy polymer.

More recently, nanoclay fillers have drawn increasing interest as it is theoretically possible to significantly improve the properties of epoxy for relatively small additive amounts.[1–20] The plausible reasons are the high aspect ratio (200–1000) and high modulus of these particles (170 GPa). Once dispersed in the matrix, the nanoclay particles create a great surface area and therefore play a key role in the confinement of the polymer chain mobility under stress.

The effect of silicate layers on mechanical properties of polymers has been widely studied. The exfoliation degree of the filler, its aspect ratio, and the developed surface affect greatly the improvement of elastic properties. Lan et al.[10] demonstrate on thermoset epoxy/amine matrix that the improvement of Young modulus is more important for silicates with higher aspect ratio. In an other work carried out by Lan and Pinnavaia[9] on elastomeric epoxy/amine matrix, it was found that modulus material increase with the length of surfactant ions. Lan et al.[10] proposed a mechanism which allows to explain the observed differences with network structure. They assumed that in the case of elastomeric matrix, the particles can align, due to deformation effect, in the direction of the stress and acting on the modulus as the same manner as fibers with high modulus. This alignment effect is minimum on glassy state because the matrix is less deformed. Pinnavaia et al.[21] multiplied the elastic modulus by 5 with incorporating 10% of organophilic montmorillonite (MMT) elaborated in their laboratory, in epoxy/amine

Correspondence to: A. Mouloud (a.mouloud@yahoo.fr).

elastomeric system as for the rigidity, the improvement of the fracture stress is more important in an elastomeric matrix than in the glassy one. Very few citations of clay nanocomposites processed with glassy epoxy-based thermoset systems. For the epoxy thermoplastic systems, several studies were reported. Boukerrou et al.[22] obtained significant increases in both the stiffness and the energy at break on epoxy-octadecylammonium modified MMT nanocomposites. The organophilic modification of clay affects the final morphology of nanocomposites on three levels. First, it allows the compatibilization of filler with the reactive mixture, then the structure of galleries after cationic exchange have an effect on the capacity of filler to be exfoliated, and finally, to affect the final morphology with using ions having specific groups. The first objective of organophilic modification is to have a guarantee that good interactions exist between the clay and the other materials (polymeric matrix and hardener). As reported in most of the related literatures,[11,12,17,19,23,24] alkylammonium ions-modified clay was used to prepare the epoxy/clay nanocomposites, which often shows a mixed structure of intercalation and exfoliation. The formation mechanism and the performance of organoclay-epoxy nanocomposites have been widely reported.[9–17,19,25] According to Pinnavaia,[10] organoclay-modified epoxies in the rubbery state at room temperature have more effective reinforcement than in the glass state. Some results revealed that organoclays could simultaneously improve both toughness and elastic moduli of epoxy resins in a similar way but more efficiently than fillers.[16,17,24] Becker et al.[19,20] found that epoxy-based nanocomposites [Nanomer I.30E with diglycidyl ether of biphenyl acetone (DGEBA) and tetraglycidyl-4,4′-diaminodiphenylmethane (TGDDM), respectively] showed increased elastic modulus and fracture toughness through the incorporation of layered silicates. Liu et al.[26] found that the I.30E in the nanocomposite was exfoliated or intercalated but was not uniformly distributed in the epoxy resin [TGDDM/4,4′-diaminodiphenyl sulfone (DDS)]. The organoclay simultaneously improved both fracture toughness K_{IC} and elastic modulus of the epoxy system without decreasing the compressive strength.

Prediction of some mechanical properties, i.e., Young modulus of composites is a common practice. Three models, i.e., Halpin Tsai, Voigt-Reuss, and Cox are suggested; these models have been already tested to evaluate the Young's modulus of epoxy nanocomposites.[27,28] The predictive models assume that the composite is composed of two phases: the matrix, in this case epoxy resin, and the particles, in this case clays. They are presented in eqs. (1)–(3), respectively:

$$E_{\mathrm{HT}} = \left[\frac{3}{8}\frac{1+2(l_c/d_c)\eta_L(1-V_c)}{1-\eta_L V_c} + \frac{5}{8}\frac{1+2\eta_T V_c}{1-\eta_T V_c}\right]E_m \quad (1)$$

$$E_{\mathrm{VR}} = \frac{3}{8}(V_c E_c + (1-V_c)E_m) + \frac{5}{8}\left(\frac{E_c E_m}{E_c(1-V_c)+E_m V_c}\right) \quad (2)$$

$$E_{\mathrm{Cox}} = \eta_o \eta_L E_c V_c + E_m(1-V_c) \quad (3)$$

where E_{HT}, E_{VR}, E_{Cox} are, respectively, the Young's modulus for the Halpin-Tsai, Voigt-Reuss, and Cox models, E_c = 170 GPa is the Young's modulus of organomontmorillonite clays,[28] E_m = 1.365 GPa is the Young's modulus of polymeric matrix (epoxy), l_c = 1 nm is the average length (thickness) of clays, d_c = 8 μm is the average diameter of clays, η_L and η_T are, respectively, the longitudinal and the transverse correction factors, η_o = 0.2, and V_c is the volume fraction of clays in the composite system. The value of the correction factor η_o depends of particles orientation degree; it has been calculated by krenchel.[29]

Note that these models make a number of assumptions.[30] They assume that the matrix and the clay particles are linear-elastic, isotropic, and that there is perfect bonding between the clays and the matrix. They also assume that the clay particles are uniform in their aspect ratio and perfectly aligned with the applied load. The models also ignore any agglomeration and particle–particle interactions.

The Halpin-Tsai model supposes that the dispersion of particles in polymeric matrix is homogeneous; the material behaves like an isotropic matter. In this model, five independent parameters are used. The expression of Voigt-Reuss model does not take into account any geometry of the reinforcement, using only three independent variables. At the origin, this model was developed to estimate the Young's modulus for a lamina of short random fibers. Cox proposes a model which is based on the modification of the rule of mixtures for the estimating of elastic modulus of composites. This model introduces the effect of the reinforcement aspect ratio into the expression of the mixture law.

The main aim of this work is to develop a glassy epoxy–amine-based nanocomposite material, with high performances particularly the mechanical properties. In this context, the effect of three different organo-modified nanoclays (two commercial products and one based on clay modified in laboratory) on morphological and mechanical behavior of glassy DGEBA epoxy resin cured with amine hardener. Thermal properties of the nanocomposites are also studied. The nanocomposites were prepared according to the *in situ* intercalation method.

EXPERIMENTAL

Materials

The DGEBA epoxy resin (GY260 as trade name) and the amine hardener (Aradur 460) were supplied

from Huntsman. The epoxy resin has a density of 1.17 g/cm^3 (at 25°C), an epoxy equivalent of 182–192 g/eq, and a viscosity range of 1200–16,000 mPa s. The amine hardener used in this study has an amine number of 240–270 mg KOH/g and a viscosity range (at 25°C) of 1800–5500 mPa s. The epoxy resin nanocomposites were prepared using a stoichiometric ratio of 100/65 (phr) between epoxy resin and hardener. The organophilic MMT clays (72T and 67G), were supplied by Laviosa Company (Italy). 72T and 67G (Dellite® 72T and Dellite® 67G as trade names, respectively) are nanoclays deriving from a naturally occurring MMT especially purified and modified with a quaternary ammonium salt (dimethyl dihydrogenated tallow ammonium, 2M2HT). The difference between them is that 67G clay is modified with relatively high amount of surfactant. BNTC18 is an organoclay prepared in the laboratory. It consists in bentonite (BNT)-type clay, from Maghnia (Algeria), modified with octadecylammonium ion by cation exchange process.[16] The properties of clay particles used in this study are summarized in Table I.

Preparation of nanocomposites

The exact amount of clay was added to a known quantity of DGEBA epoxy resin in a beaker and stirred by hand for about 2 min. Then the mixture was immersed in a water bath at 40°C for 1 h with mechanical stirring at about 1000 revolution per minute (rpm). After that, the hardener was added to the resulting suspension, and maintained for another 1 h at 40°C with mechanical stirring. The mixture was then degassed under vacuum for few minutes inside an oven, poured into an aluminum mould, and cured in the first time during 24 h at ambient temperature. Then it was postcured at 120°C for 3 h. At least six test specimens were machined from each casting panel for mechanical evaluation.

TABLE I
Properties of Clay Particles

Properties	72T	67G	BNTC18
Specific density[a]	1.7	1.7	2.3
Mean particle size[a] (μm)	8–9	8–9	8–9
XRD basal spacing[b] (Å)	26.6	34.3	32.1
Specific surface[c] $^{(BET)}$ (m^2/g)	115	78	98
Organic Modifier[d] (%)	38	42	22
CEC[e] (meq/100 g)	101	97	103

[a] Commercial data (Laviosa Company).
[b] Measured by XRD.
[c] Measured by porosimetry (BET method).
[d] Measured by TGA.
[e] Determined from the values of the fire loss after the calcination at 1050°C during 2 h carried out by X-ray fluorescence.

Nanocomposites characterization

The degree of intercalation/exfoliation and the *d*-spacing between clay platelets were investigated using X-ray diffraction (XRD) analysis. XRD analyses were performed using a FR591 Bruker AXS X-ray generator with a monochromatic Cu Kα radiation (λ = 1.541 Å) and linear collimation. X-ray patterns were collected with a Mar345 Image-Plate detector (Marresearch, Norderstedt, Germany) mounted on a rotating anode X-ray generator FR591 (Bruker, Courtaboeuf, France) operated at 50 kV and 50 mA. The monochromatic Cu K_α radiation (k = 1.541 Å) was focalized with a 350-μm focal spot at 320 mm by a double reflection on an elliptic cross multilayer Montel mirror (Incoatec, Geesthacht, Germany). The beam was defined under vacuum by four motorized carbon–tungsten slits (JJ-Xray, Roskilde, Denmark) positioned in front of the mirror (500 μm).

Transmission electron microscopy (TEM) was used to confirm the nanoscale morphology of the nanocomposite cured samples. Concerning TEM analyses, a JEOL JEM-1400 electron microscope was used. The observations were performed at an acceleration voltage of 100 kV. The ultrathin TEM samples with a thickness of 70 nm were cut using an ultramicrotome Leica ultracut UCT at room temperature.

The glass transition temperatures of the nanocomposites were determined after second heating using a Pyris 1 differential scanning calorimeter (DSC) from PerkinElmer. Samples of about 10 mg were sealed in aluminum pans and heated from 25 to 100°C at a heating rate of 10°C/min under nitrogen atmosphere.

Tensile tests were performed on an MTS universal test machine, Synergie RT/1000, at 23°C and 1 mm/min crosshead speed. A clip type of extensometer (nominal length of 25 mm) was used to measure strain within the specimen gauge length. At least six specimens of each composition were tested.

The impact strength of the nanocomposites was performed using a Tinius Olsen apparatus type Impact 503 with a pendulum of 2.7 J and 609 mm length. The speed of pendulum was 3.46 m/s. Radius V notched samples (45 ± 1°) were used in this test. The notch depth and its radius at the base were 1 mm and 0.25 ± 0.05 mm, respectively. The test is performed according to ASTM D256-97.[31] The specimen dimensions were 65 × 15 × 4 mm^3. At least eight test specimens were tested for each composition.

The mode I fracture toughness is measured in terms of critical stress intensity, K_{IC}. Fracture toughness values were determined using precracked, single edge-notched specimens in three point bending with 50-mm span distance. The specimen dimensions were the same as those used for the impact

strength test. The tests were performed on at least six specimens for each composition at room temperature using an MTS universal machine, Synergie RT/1000 type, with a crosshead speed of 5 mm/min. The critical stress intensity factor, in units of MPa $m^{1/2}$, was determined according to ASTM E 399 – $06^{\epsilon 2}$, using the following relationship:[32]

$$K_{IC} = \frac{3PS\sqrt{a}}{2BW} Y \quad (4)$$

where P is the load at failure, S the length of the span, a the precrack length, B the thickness of specimen, W the width of specimen, and Y a shape factor given by:

$$Y = 1.93 - 3.07(a/W) + 14.53(a/W)^2 - 25.11(a/W)^3 + 25.80(a/W)^4 \quad (5)$$

Analysis of the fracture surfaces of impacted samples was also performed using a scanning electron microscope (SEM) FEI, Quanta-600 type at 20 kV. Before SEM observations, the fracture surfaces were coated with a thin layer of gold.

RESULTS AND DISCUSSION

Morphology

The morphology of the materials was studied by XRD and TEM analyses. Figure 1 shows the XRD spectrums of pure 72T, 67G, and BNTC18 organoclays; the basal spacing d_{001} are 26.6, 34.3, and 32.1 Å, respectively.

Figure 2 shows the XRD patterns of the epoxy/clay nanocomposites with various clay contents. Globally, the structures of the nanocomposites are similar. The peaks representing the basal spacing of nanoclays in the nanocomposites are shifted to lower values of 2θ angle, corresponding to d-spacing of 37.9, 38.5, and 44.1 Å, respectively, for 72T, 67G, and BNTC18 systems when mixed with epoxy to form the nanocomposite materials. This indicates that single or double layers of epoxy polymer chains could have been intercalated between the

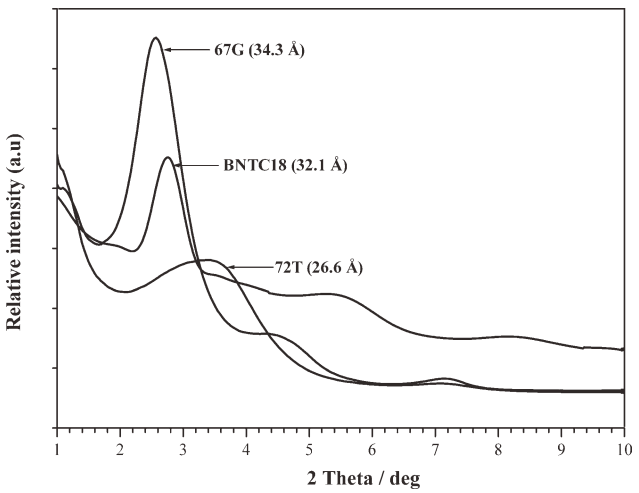

Figure 1 XRD traces of pure clays.

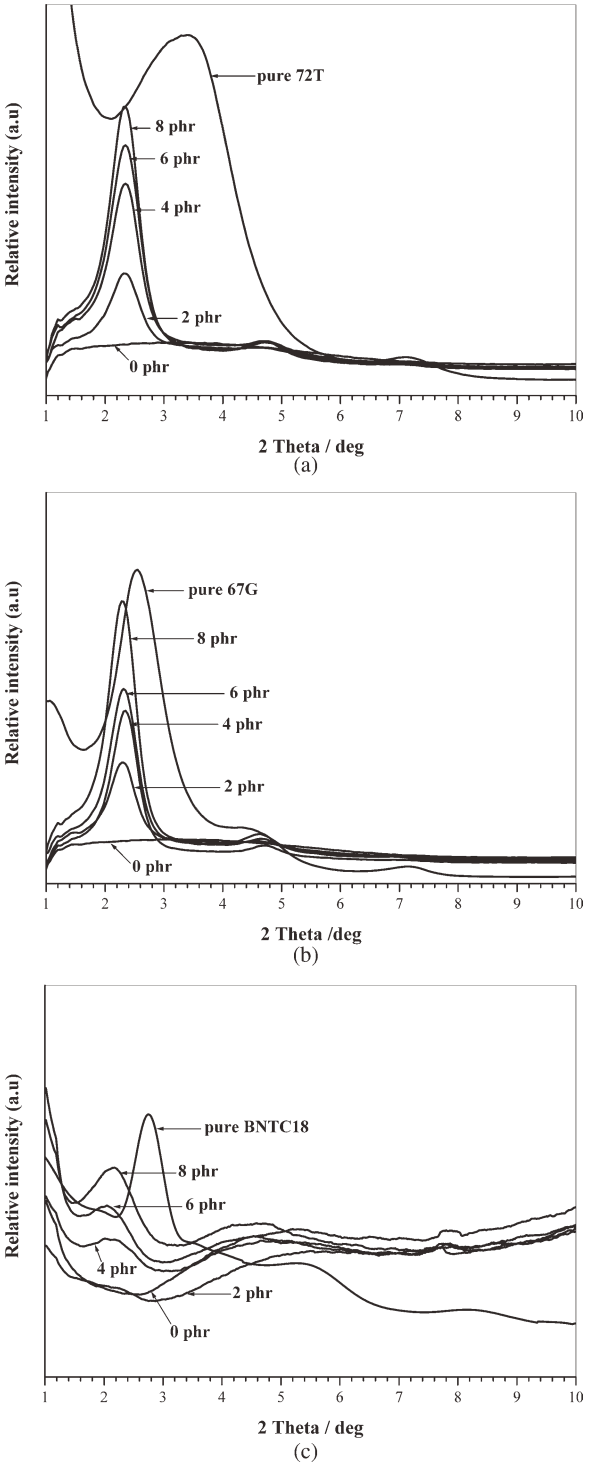

Figure 2 XRD patterns of the epoxy/clay nanocomposites with (a) 72T, (b) 67G, and (c) BNTC18.

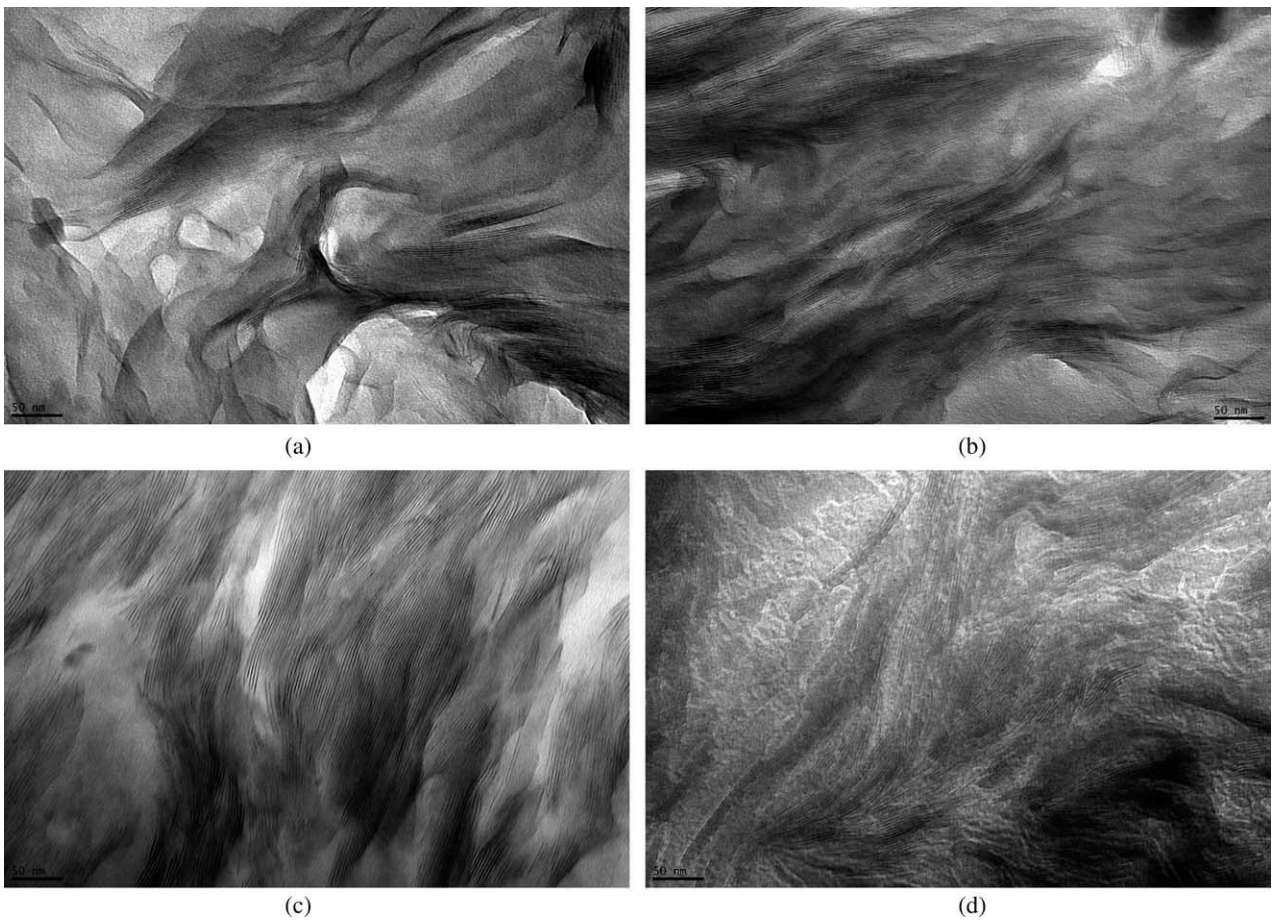

Figure 3 High-magnification TEM images of nanocomposites based on different clays: (a) 72T/4 phr, (b) 67G/4 phr, (c) BNTC18/4 phr, and (d) BNTC18/2 phr.

organo-functionalized clay nanolayers during mixing. The nanocomposite with 2 phr content of BNTC18 clay does not show, however, any peak of a diffraction corresponding to (001) plane, this is attributed in general to two possible reasons: (a) exfoliated structure, or (b) disordered intercalated structure. This can be further confirmed by TEM observation as shown in Figure 3. In the other hand, it is interesting to note that the higher excess of organic modifier has no effect on exfoliating the clay nanolayers in epoxy matrix.

Nanocomposites superstructures were investigated by means of TEM to visually evaluate the degree of intercalation and the amount of aggregation of clay clusters. Typical TEM images are displayed in Figure 3. In this figure (images a, b, and c) are exhibited TEM images of 72T, 67G, and BNTC18 clays-based nanocomposites with 4 phr clay content, respectively. Image d in Figure 3 shows TEM image of BNTC18 nanocomposite with 2 phr content. In the case of the 4 phr of clay content, it is clear that the dispersion of the clays in the epoxy matrix is in the intercalate form for all nanocomposites. In the intercalated system, the silicates retain much of their face-to-face alignment and can be seen to cluster together in large domains ranging from a few hundred nanometers to micrometers in size. Similar results are reported elsewhere.[24,33] The 2 phr content with BNTC18 show a structure which can be attributed to a disordered intercalate morphology rather than complete exfoliation. TEM observations confirm globally the XRD analyses.

Thermal properties

Figure 4 is a plot of the glass transition temperatures (T_g) versus the clay content as obtained from DSC measurements. T_g of the neat epoxy is around 65°C. DSC measurement revealed the same shape of thermal behavior in term of T_g results in the case of nanocomposites prepared with 72T and 67G clays. In fact, both for these two clays, we can observe a slight decrease in the T_g value when adding nanoclays. This decrease in the T_g temperature can be explained by the role played by the clays in the nanocomposite mixture. Organoclays allow the sliding of macromolecular chains with respect to each other; thus, this increases the flexibility of the

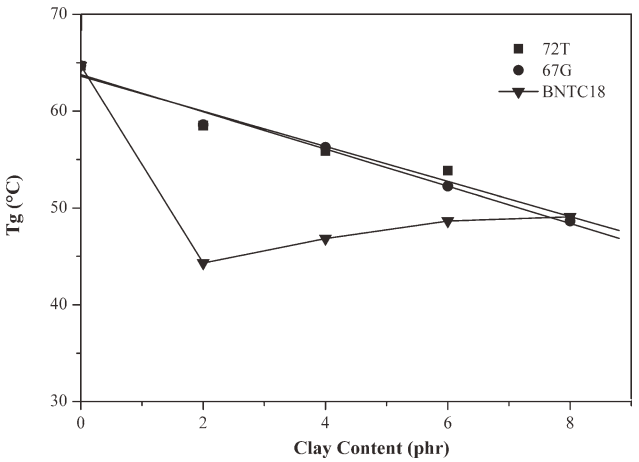

Figure 4 T_g results of epoxy nanocomposites as a function of clay content.

obtained material and is an advantage to obtain tougher nanocomposites. The reduction in T_g was found to be in the order of 24% for 72T- and 67G-based nanocomposites at 8 phr clay content. Similar results have been reported elsewhere.[24,34–36] However, for BNTC18-based nanocomposites, the T_g dropped significantly with addition of just 2 phr of BNTC18 clay (reduction of 31%), then leveling off for high nanoclay contents.

This behavior for BNTC18-based nanocomposites is different from that of the two other clays; this might be explained by the role played by the clay organic modifier, which is in this case octadecylammonium ion, whereas in the case of 72T and 67G, these two clays are modified by dimethyl dihydrogenated tallow ammonium (2M2HT). Zilg et al.[24,37] have found similar results in this context. A significant decrease of the T_g was observed for intercalated epoxy nanocomposites based on protonated primary amines, and functionalized ternary amines with respect to those of nanocomposites based on layered silicates modified with nonfunctionalized quaternary ammonium chloride. It indicates that effective intercalation and interfacial coupling affects the epoxy network and lowers glass temperatures. The effect of the organoclay on the α-relaxation or glass transition temperature (T_g) of DGEBA-based epoxy nanocomposites has been the subject of numerous studies. In some cases, a constant or increased T_g has been reported with increasing organoclay addition.[12,25,38–41] Messersmith and Giannelis[12] have used an epoxy DGEBA type with different curing agents based on anhydride and amine types and an organo-modified mica-type silicate, the organic modifier used is bis(2-hydroxy ethyl) methyl tallow-alkyl ammonium chloride. The nanocomposite exhibited a broadened T_g at slightly higher temperature than the unmodified epoxy. In Massam and Pinnavaia[25] study, epoxy–clay nanocomposites have been prepared by the reaction of a DGEBA epoxy resin and polyoxyalkylene amine curing agent in the presence of MMT modified with octadecylammonium ion. They found an increase of T_g with organo-MMT concentration. Brown et al.[38] used a DGEBA epoxy resin type and polyoxypropylene diamine (Jeffamine D2000 and Jeffamine D400) as curing agent. The clay used in the study was MMT modified with three different organic modifiers based on hydroxyl-substituted quaternary ammonium ions. An increase in T_g was observed with clay content. For Lee and Lichtenhan[39] work, a mixture of two types of epoxy resin was used: DGEBA and 1,4-butanediol diglycidylether. The curing agent used was a mixture of the diamine-terminated polypropylene oxide of different molecular weight (Jeffamine D230 and D2000). Octadecylammonium ion was used as organic modifier for MMT clay. Because of the presence of clay reinforcements, no changes for the T_g of the nanocomposites were observed. Kelly et al.[40] used a DGEBA epoxy resin with a polyamine (V-40) as curing agent. Three MMTs were used in this work. They include MMTs with organic cations derived from (a) tyramine hydrochloride, (b) aminolauric acid, and (c) polyamide. The T_g of the epoxy nanocomposites was observed to increase when increasing organo-modified MMT concentration. Chen and Yang[41] used a DGEBA epoxy resin type with two curing agents nadicmethyl anhydride and benzyldimethylamine. Alkylamines (C12 and C18), aminocarboxylic acids (C6 and C12), and diamines (C6 and C12) were used as organic modifiers for MMT. The addition of organo-modified MMT to epoxy showed higher T_g for the obtained nanocomposite. Others have found a reduction in the glass transition temperature with increasing organosilicate content. It was reported that highly crosslinked and high glass transition temperature resin systems led to a steady decrease in T_g with increasing organo-ion concentration.[16,19] Kornmann et al.[16] used in their study epoxy-layered silicate nanocomposites based on TGDDM resin cured with DDS. Fluorohectorites modified by means of interlayer exchange of sodium cations for protonated dihydroimidazolinzes and octadecylamine were used. A decrease in the T_g was observed for all the nanocomposites. Becker et al.[19] studied three different epoxy resins: bifunctional DGEBA, trifunctional triglycidyl *p*-amino phenol, and tetrafunctional TGDDM. All resins were cured with diethyltoluene diamine. Octadecylammonium ion was used to modify MMT clay. It was found that the presence of organoclay steadily decreased T_g temperature with increasing clay concentration.

The complexity of the cure reaction and possible side reactions involved made it difficult to determine the governing factor causing the reduction in T_g. The crosslink density in the filled systems may

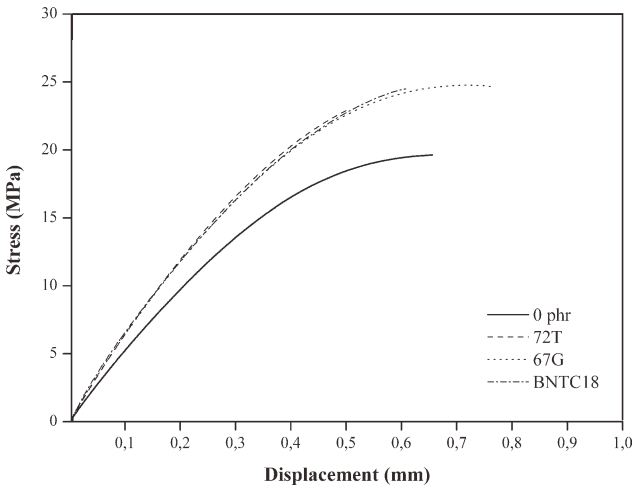

Figure 5 Example of tension curves of non charged epoxy and with 4 phr of different clays.

be decreased or the matrix plasticized by smaller molecules present in the network.[8] The organoclay may catalyze epoxy etherification and unreacted entrapped resin, hardener, or compatibilizer molecules may act as a plasticizer. In addition, the high cure temperatures required for these resin systems may degrade the layered silicate surface modifier, which are nominally stable to about 200–250°C. Chen et al.[42] found a decreased T_g for an hexahydro-4-methylphtalic anhydride cured epoxy (3,4-epoxycyclohexylmethyl-3,4-epoxycyclohexane)-layered silicate nanocomposite. The layered silicate was rendered organophilic through bis(2-hydroxyethyl) methyl tallow alkylammonium cations. The decrease in T_g was proposed to be due to the formation of an interphase consisting of the epoxy resin, which is plasticized by the surfactant chains. Triantafillidis et al.[43] reported that limiting the clay modification reduces the plasticizing effect due to the organic modifier.

Mechanical properties

Figure 5 represents typical stress-displacement curves of amine-cured neat epoxy and related clay nanocomposites loaded with 4 phr of various clays. From these curves, the elastic behavior of the nanocomposite materials is clearly observable, and the tensile modulus increases with clay content. Note that the tensile strength is not quoted here, as this parameter is highly dependent on the surface finish of the specimens, for brittle materials such as it is the case of this study.

The variation of elastic modulus as a function of clay content is shown in Figure 6. As it can be seen, the elastic modulus of the nanocomposites increases continuously with increasing clay content. Similar results have been obtained elsewhere.[9,33,36,44–47] The higher values are observed in the case of nanocomposites manufactured with BNTC18 clay at all loading clays. Up to 4 phr, the 67G/epoxy shows higher increase than the 72T/epoxy nanocomposite; then at higher clay contents, the increase in modulus is more important for the 72T/epoxy nanocomposite. A maximum of about 35% improvement is observed when adding 8 phr BNTC18 clay. Although this improvement is not considerable compared to results obtained in other studies related to epoxy nanocomposites, it is important here to note that the enhancement of the tensile modulus is interesting in spite of its low rate. The better improvement of elastic modulus in BNTC18/epoxy compared to 72T/epoxy and 67G/epoxy can be attributed to the good dispersion of the nanoparticles in the epoxy matrix for this case, because this restricts the mobility of polymer chains under loading, as well as to the good interfacial adhesion between the nanoclays and the epoxy matrix.[48] The orientation of clay platelets and polymer chains with respect to the loading direction can also contribute to the reinforcement effects.[49] However, it can also be observed that the decreasing rate of elastic modulus improves at higher clay concentration for all nanocomposites systems; this can be attributed to the presence of unexfoliated aggregates in the structure of the resin.[49]

Figures 7, 8, and 9 show the changes of Young's modulus of amine-cured epoxy/clay nanocomposites as a function of the volume fraction of the clays for 72T, 67G, and BNTC18 systems respectively. For theoretical predictions, the Halpin-Tsai, the Voigt-Reuss, and the Cox models are used. From these different theories, it appears that at low clay content, the Cox model is the closest to the experimental values concerning the 72T- and 67G-based nanocomposites, whereas for BNTC18-based nanocomposites,

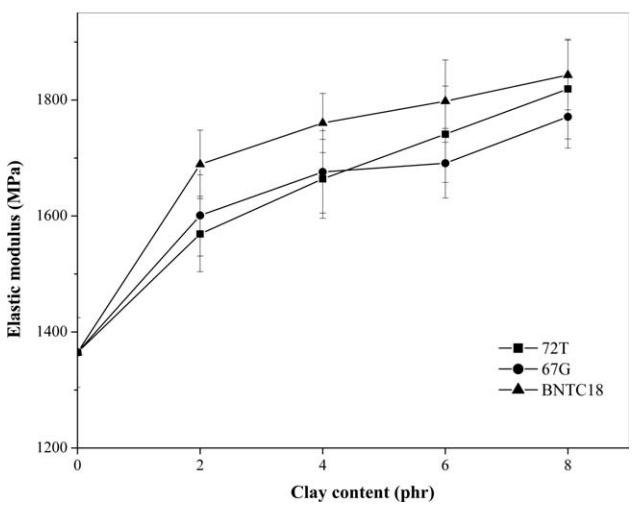

Figure 6 Young's modulus of amine-cured epoxy/clay nanocomposites with different clay content.

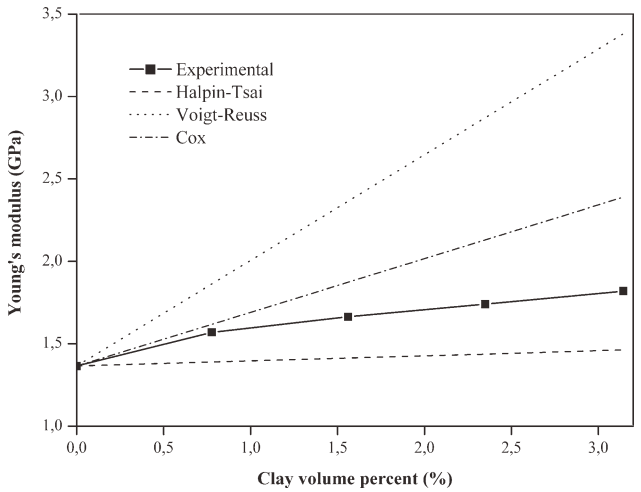

Figure 7 Young's modulus (E) of amine-cured epoxy/72T clay nanocomposites with changing clay content.

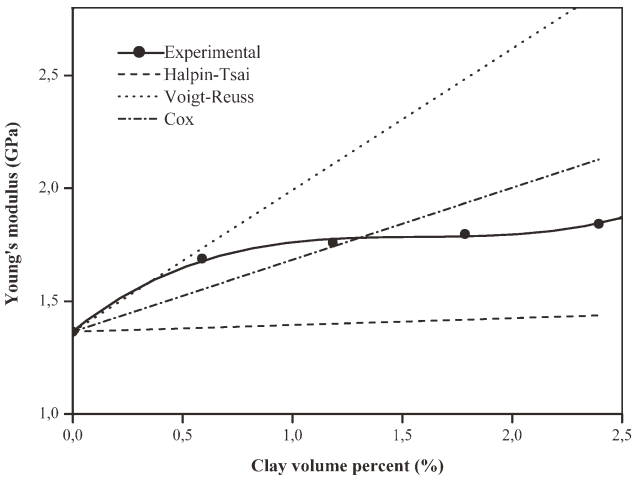

Figure 9 Young's modulus (E) of amine-cured epoxy/BNTC18 clay nanocomposites with changing clay content.

the Voigt-Reuss model is the closest one. At relatively higher content of 0.8–3.1 vol %, the results of 72T- and 67G-based nanocomposites show the same trends like Halpin-Tsai model but the experimental values of tensile modulus are higher by 0.3 GPa. Whereas for the BNTC18-based nanocomposites, at 0.6–2.4 vol % content, the Cox model is the closest one relatively with the experimental values (average difference of 0.3 GPa with experimental). It can be observed that nanocomposites based on 72T and 67G clays have similar response with these models, at high clay content as well as at low content. Whereas BNTC18 clay-based nanocomposites have a different behavior. This result confirm the thermal behavior (T_g) for these materials, and it seems that the nature of organic modifier of clays plays an essential role in this behavior, owing the fact that 72T and 67G are modified by the same organic modifier (2M2HT). Whereas BNTC18 clay is modified by another type of organic modifier (octadecylammonium).

The effect of adding nanoclays on the notched izod impact strength of the specimens is shown in Figure 10. Impact strength of the composites increases with clay loading at low concentration; similar results have been reported elsewhere.[46,50–52] The clay particles seem to act as crack stoppers and form tortuous crack propagation path, resulting in higher impact energy. The maximum improvements of impact strength are obtained with 2 phr of clay content. For example, at this concentration, an increase rate of 77 and 65% is obtained, respectively, with 72T and BNTC18 clays, whereas 53% of improvement is obtained with 67G clay. The improvement of the impact strength at low clay content may be attributed to the agglomeration of the particles clays at high clay concentration, as it can be seen in SEM micrographs of Figure 11.

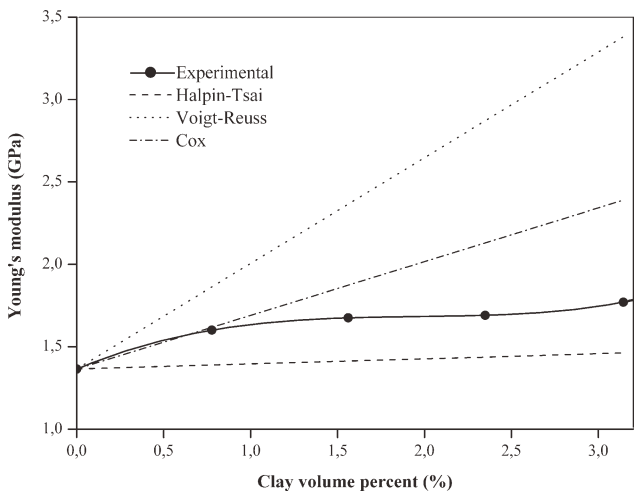

Figure 8 Young's modulus (E) of amine-cured epoxy/67G clay nanocomposites with changing clay content.

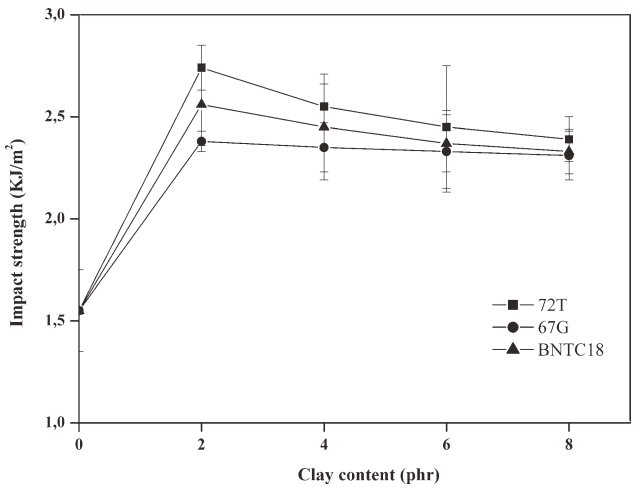

Figure 10 Variation of impact strength of epoxy/clay nanocomposites with different clay content.

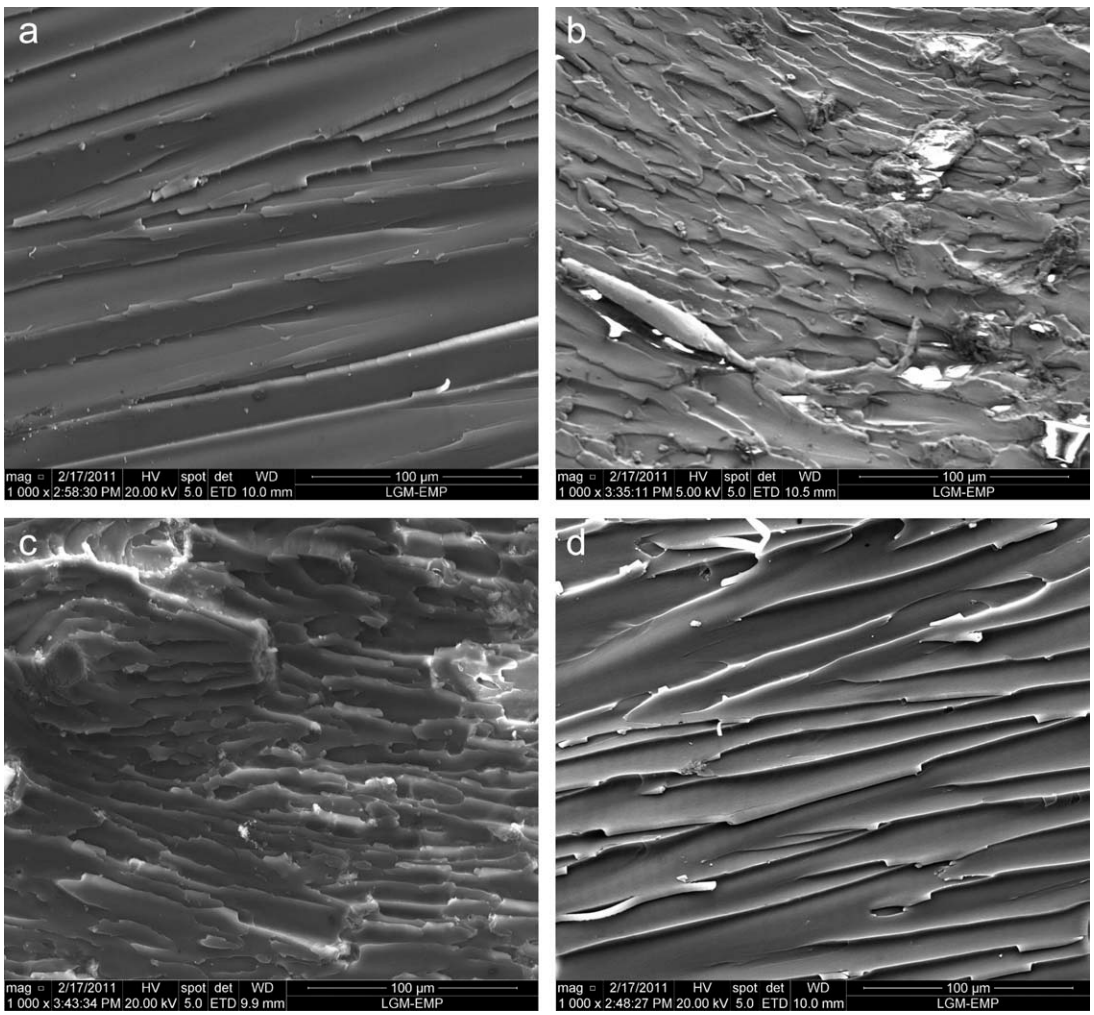

Figure 11 SEM micrograph of fracture surface of the neat epoxy and its nanocomposites with 2 phr of clay. (a) Neat epoxy, with (b) 72T clay, (c) 67G clay, and (d) BNTC18 clay.

The improvement of impact properties of nanocomposites is supported by the fracture surface studies. Fracture surface of the neat composite [Fig. 11(a)] is quite smooth and flat compared to that of the nanoclays-DGEBA resins; this indicated brittle fracture behavior, corresponding to poor impact strength.[53] This smooth pattern completely disappeared and rough fracture surfaces appear upon addition of organoclays to epoxy. Throughout the micrographs, it can be seen that there is an increase in the roughness of the fracture surfaces and tortuous path. In fact, the apparent roughness of the fracture surfaces varies significantly from one composite to another, depending on the type of the silicate used. Similar results have been already reported in litterature.[30] The fracture surfaces of epoxy–clay nanocomposites show massive shear deformation. Energy is absorbed for such shear yielding, leading to the increase in impact strength.[54] This explains why epoxy–clay nanocomposites show higher impact strength compared to the unmodified composite. The main toughening effect is due to debonding and subsequent plastic deformation of the epoxy polymer around the particles, as observed by SEM.[30]

Results concerning the K_{IC} values are shown in Figure 12. It can be seen that at a low concentration of 2 phr, there is a significant jump of the critical stress intensity factor for the 72T- and 67G-based nanocomposites, whereas the maximum of K_{IC} is obtained at 4 phr content for BNTC18-based nanocomposites. Similar results have been reported elsewhere.[17,36,55,56] It is also observed that the fracture toughness improved more for 72T and 67G nanocomposites than BNTC18 ones. The high improvement is globally obtained with 72T-based nanocomposites for all concentrations. The improvement rate in fracture toughness reaches about 90% in the case of 72T-based nanocomposites for the concentration of 2 phr, comparatively to the neat epoxy, whereas 57 and 29% of improvement have been obtained, respectively, for 67G and BNTC18. However, the values of K_{IC} dropped with further addition of clays;

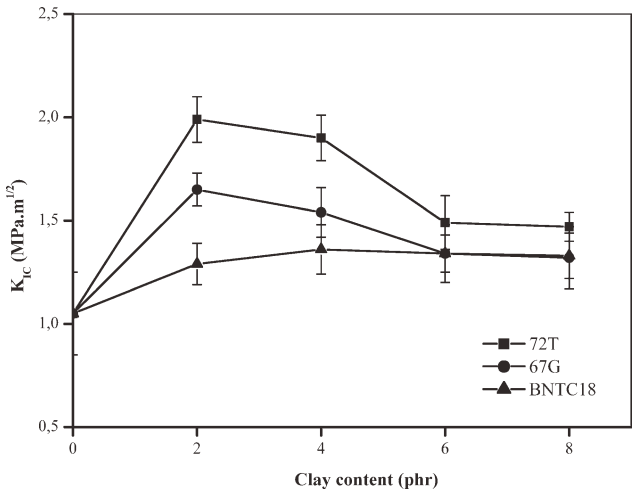

Figure 12 Dependence of fracture toughness of epoxy/clay nanocomposites on clay concentration.

the agglomeration of clay particles like-tactoids is mainly the reason for this drop. The nanocomposites elaborated with organoclays in this work exhibited an intercalative structure as shown by XRD and TEM analyses, and this is in good agreement with results obtained by Zilg et al.,[24] who proposed that intercalated clay promotes toughness whereas exfoliated clay platelets mainly improve stiffness of the polymer matrix, due to energy-absorbing shearing of intercalated clay layers. Furthermore, due to lateral dimension of materials, which is in the micron scale, this may encourage crack stopping and pinning. It can also be noticed that for 72T and 67G, the max K_{IC} is reached at 2 phr, then followed by a sharp decrease before leveling off. This might be attributed to some clay agglomeration which might act as stress concentrator and lead to this relative decrease. At the contrary, K_{IC} of BNTC18 nanocomposite reached a maximum at 4 phr then levels off. Agglomeration, if any, does not seem to affect the K_{IC} as well as the impact strength.

Critical strain energy release rates G_{IC} is calculated from the stress intensity values using the following relationship:

$$G_{IC} = \frac{K_{IC}^2}{E}(1-\nu^2) \quad (6)$$

where E is the Elastic modulus, ν the Poisson's ratio and a typical value of 0.33 was used in this study.[57] The dependence of G_{IC} of epoxy/clay nanocomposites on clay concentration represented in Figure 13 follows the same trend as K_{IC}. As for K_{IC}, there is a significant jump of G_{IC} by adding 2 phr of 72T and 67G clays; the enhancement ratios at this critical content are 212 and 110%, respectively. Whereas a little increase is relatively observed with BNTC18 clay (30%). As G_{IC} represents the energy per unit area necessary to create a new surface area at the crack tip, such a significant enhancement of G_{IC} indicates that the fracture resistance is considerably improved. After that, the values of G_{IC} dropped considerably with further addition of clay with similar behavior as for K_{IC}.

CONCLUSIONS

A series of glassy nanocomposite material were prepared by addition of organoclays into the epoxy-amine matrix with mechanical stirring. The effect on morphological and mechanical behaviors of the obtained nanocomposites was investigated by means of various tests. Based on the results obtained and discussed previously, the following conclusions can be drawn:

- The epoxy/clay nanocomposites with intercalated structure have been obtained. The structure of organically modified clay platelets depends on the technique used to achieve the dispersion and on the cure conditions (temperature and cycle time).
- The addition of organically modified nanoclays platelets according to operative conditions and processing used here (mechanical stirring) improve mechanical performances such as elastic modulus, impact strength, and fracture toughness of DGEBA epoxy resin. This improvement is obtained at low clay concentration (optimal content around 2 phr). Around this clay concentration, theoretical predictions of the nanocomposites moduli were in good agreement with experimental values. It was found that at a low content of 2 phr (1.2 wt %) of nanoclays, the impact strength and the fracture toughness were improved by 77 and 90%, respectively, comparatively to the neat epoxy.

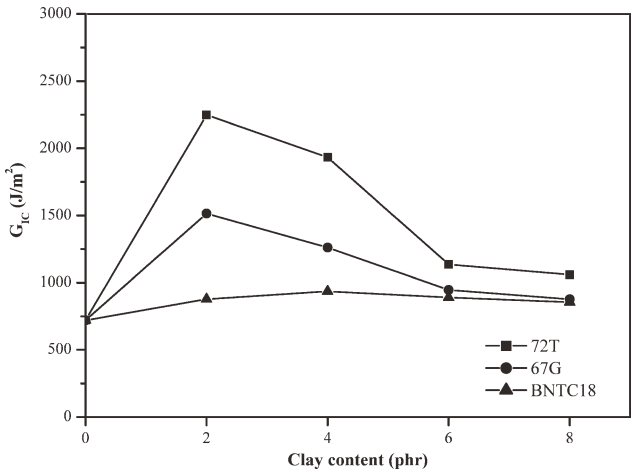

Figure 13 Dependence of critical strain energy release rates of epoxy/clay nanocomposites on clay concentration.

- It has been confirmed that the structure of such nanocomposites is directly related to the fracture behavior of the material; it appears that fracture toughness may be associated with these types of structures that are formed under the present processing conditions.
- Globally, it was also found that, T_g decreases when the nanoclays content increases; leading to more flexible material and tougher nanocomposites.
- Because of the ease of molding method applied in this work, the nanoclays concentration should be kept around 2 phr to get good mechanical properties.

The authors thank Professor Yves Grohens and his research team at the Materials Engineering Laboratory of Bretagne, Research Centre – France (LIMATB), European University of Britanny for material help and technical assistance during this work. Laviosa Compagny (Italy) is also gratefully acknowledged for providing the clays.

References

1. Sudhakara, P.; Kannan, P.; Obireddy, K.; Varada Rajulu, A. J Mater Sci 2011, 46, 2778.
2. Zainuddin, S.; Hosur, M. V.; Zhou, Y.; Narteh, A T.; Kumar, A.; Jeelani, S. Mater Sci Eng A 2010, 527, 7920.
3. Gârea, S.-A.; Iovu, H.; Voicu, G. Appl Clay Sci 2010, 50, 469.
4. Lim, S. R.; Chow, W. S. Polym-Plast Technol Eng 2011, 50, 2, 182.
5. Korobko, A. P.; Krasheninnikov, S. V.; Levakova, I. V.; Drozd, S. N.; Chvalun, S. N.; Nikolaev, V. V.; Shcherbina, M. A.; Cherdyntseva, S. V. Polym Sci Ser A 2011, 53, 75.
6. Choi, Y. Y.; Lee, S. H.; Ryu, S. H. Polym Bull 2009, 63, 47.
7. Gârea, S.-A.; Nicolescu, A.; Deleanu, C.; Iovu, H. Int J Polym Anal Char 2010, 15, 497.
8. Zaarei, D.; Sarabi, A. A.; Sharif, F.; Gudarzi, M. M.; Kassiriha, S. M. J Dispersion Sci Technol 2010, 31, 1350.
9. Lan, T.; Pinnavaia, T. J. Chem Mater 1994, 6, 2216.
10. Lan, T.; Kaviratna, P. D.; Pinnavaia, T. J. Chem Mater 1995, 7, 2144.
11. Wang, Z.; Pinnavaia, T. J. Chem Mater 1998, 10, 1820.
12. Messersmith, P. B.; Giannelis, E. P. Chem Mater 1994, 6, 1719.
13. Tolle, T. B.; Anderson, D. P. Compos Sci Technol 2002, 62, 1033.
14. Kornmann, X.; Lindberg, H.; Berglund, L. A. Polymer 2001, 42, 1303.
15. Kornmann, X.; Lindberg, H.; Berglund, L. A. Polymer 2001, 42, 4493.
16. Kornmann, X.; Thomann, R.; Mulhaupt, R.; Finter, J.; Berglund, L. A. Polym Eng Sci 2002, 42, 1815.
17. Zerda, A. S.; Lesser, A. J. J Polym Sci: Part B 2001, 39, 1137.
18. Triantafillidis, C. S.; LeBaron, P. C.; Pinnavaia, T. J. J Solid State Chem 2002, 167, 354.
19. Becker, O.; Varley, R.; Simon, G. Polymer 2002, 43, 4365.
20. Becker, O.; Varley, R.; Simon, G. P. Eur Polym J 2004, 40, 187.
21. Pinnavaia, T. J.; Lan, T.; Wang, Z.; Shi, H.; Kaviratna, P. D. ACS Symp Ser Nanotechnol 1996, 622, 250.
22. Boukerrou, A.; Duchet, J.; Fellahi, S.; Kaci, M.; Sautereau, H. J Appl Polym Sci 2007, 103, 3547.
23. Manias, E.; Han, W. J.; Jandt, K. D.; Kramer, E. J.; Giannelis, E. P. Materials Research Society Symposium Proceeding, Issue: Nanophase and Nanocomposite Materials II, Boston, USA, 1997, 457, 495.
24. Zilg, C.; Mulhaupt, R.; Finter, J. Macromol Chem Phys 1999, 200, 661.
25. Massam, J.; Pinnavaia, T. J. Mat Res Soc Symp Proc 1998, 520, 223.
26. Liu, W.; Hoa, S. V.; Pugh, M. ICCM-14, San Diego, California, USA; 2003, p 14.
27. Guzman de Villoria, R.; Miravete, A. Acta Mater 2007, 55, 3025.
28. Miyagawa, H.; Rich, M. J.; Drzal, L. T. J Polym Sci Part B: Polym Phys 2004, 42, 4391.
29. Garrigue, J. Statique des solides élastiques en petites déformations, Ecole Supérieure de Mécanique de Marseille, Marseille, France, 2001.
30. Kinloch, A. J.; Taylor, A. C. J Mater Sci 2006, 41, 3271.
31. ASTM Standard D256-97. "Standard test methods for determining the izod pendulum impact resistance of plastics", ASTM International, West Conshohocken, PA, 1997.
32. ASTM E 399 – $06^{\varepsilon 2}$ "Standard test method for linear-elastic plane-strain fracture toughness KIC of metallic materials", ASTM International, West Conshohocken, PA, 2008.
33. Yasmin, A.; Luo, J. J.; Abot, J. L.; Daniel, I. M. Compos Sci Technol 2006, 66, 2415.
34. Akbari, B.; Bagheri, R. Eur Polym J 2007, 43, 782.
35. McIntyre, S.; Kaltzakorta, I.; Liggat, J. J.; Pethrick, R.; Rhoney, A. I. Ind Eng Chem Res 2005, 44, 8573.
36. Wang, L.; Wang, K.; Chen, L.; Zhang, Y.; He, C. Compos Part A: Appl Sci Manufact 2006, 37, 1890.
37. Zilg, C.; Thomann, R.; Finter, J.; Mülhaupt, R. Macromol Mater Eng 2000, 280-281, 41.
38. Brown, J. M.; Curliss, D.; Vaia, R. A. Chem Mater 2000, 12, 3376.
39. Lee, A.; Lichtenhan, J. D. J Appl Polym Sci 1999, 73, 1993.
40. Kelly, P.; Akelah, A.; Qutubuddin, S.; Moet, A. J Mater Sci 1994, 29, 2274.
41. Chen, K. H.; Yang, S. M. J Appl Polym Sci 2002, 86, 414.
42. Chen, J. S.; Poliks, M. D.; Ober, C. K.; Zhang, Y.; Wiesner, U.; Giannelis, E. P. Polymer 2002, 43, 4895.
43. Triantafillidis, C. S.; LeBaron, P.; Pinnavaia, T. J. Chem Mater 2002, 14, 4088.
44. Qi, B.; Zhang, Q. X.; Bannister, M.; Mai, Y. W. Compos Struct 2006, 75, 514.
45. Xidas, P. I.; Triantafyllidis, K. S. Eur Polym J 2010, 46, 404.
46. Basara, C.; Yilmazer, U.; Bayram, G. J Appl Polym Sci 2005, 98, 1081.
47. Yasmin, A.; Abot, J. L.; Daniel, I. M. Scripta Mater 2003, 49, 81.
48. Wei, C. L.; Zhang, M. Q.; Rong, M. Z.; Friedrich, K. Compos Sci Tech 2002, 62, 1327.
49. Liu, X.; Wu, Q. Polymer 2001, 42, 10013.
50. Wang, B.; Qi, N.; Gong, W.; Li, X. W.; Zhen, Y. P. Radiat Phys Chem 2007, 76, 146.
51. Mohan, T.; Kumar, M. R.; Velmurugan, R. J Mater Sci 2006, 41, 5915.
52. Ratna, D.; Manoj, N. R.; Varley, R.; Raman Singh, R. K.; Simon, G. P. Polym Int 2003, 52, 1403.
53. Velmurugan, R.; Mohan, T. P. J Mater Sci 2004, 39, 7333.
54. Kinloch, A. J.; Young, R. J. Fracture Behaviour of Polymers; Applied Science: London, 1983.
55. Fröhlich, J.; Golombowski, D.; Thomann, R.; Mülhaupt, R. Macromol Mater Eng 2004, 289, 13.
56. Kim, B. C.; Park, S. W.; Lee, D. G. Compos Struct 2008, 86, 69.
57. Barbero, E. J. Materials, Introduction to Composite Materials Design,Vol.17; Taylor & Francis: New York, 1999.